A P_{IIB}-type Ca^{2+}-ATPase is essential for stress adaptation in *Physcomitrella patens*

Enas Qudeimat[a], Alexander M. C. Faltusz[a], Glen Wheeler[c], Daniel Lang[a], Hauke Holtorf[b], Colin Brownlee[c], Ralf Reski[a,d,e], and Wolfgang Frank[a,d]

[a]Plant Biotechnology, Institute of Biology II, Faculty of Biology, [d]Freiburg Initiative for Systems Biology, Faculty of Biology, and [e]Centre for Biological Signaling Studies, University of Freiburg, Schänzlestrasse 1, 79104 Freiburg, Germany; [b]Biotechnologisches Gymnasium, Albert-Schweitzer-Schule, 78048 Villingen-Schwenningen, Germany; and [c]Marine Biological Association of the United Kingdom, Citadel Hill, Plymouth PL1 2PB, United Kingdom

Edited by Mark Estelle, Indiana University, Bloomington, IN, and approved October 23, 2008 (received for review January 28, 2008)

Transient cytosolic Ca^{2+} ($[Ca^{2+}]_{cyt}$) elevations are early events in plant signaling pathways including those related to abiotic stress. The restoration of $[Ca^{2+}]_{cyt}$ to prestimulus levels involves ATP-driven Ca^{2+} pumps, but direct evidence for an essential role of a plant Ca^{2+}-ATPase in abiotic stress adaptation is missing. Here, we report on a stress-responsive Ca^{2+}-ATPase gene (*PCA1*) from the moss *Physcomitrella patens.* Functional analysis of *PCA1* in a Ca^{2+} transport-deficient yeast mutant suggests that *PCA1* encodes a P_{IIB}-type Ca^{2+}-ATPase harboring an N-terminal autoinhibitory domain. In vivo localizations identified membranes of small vacuoles as the integration site for a PCA1:GFP fusion protein. *PCA1* mRNA levels are up-regulated by dehydration, NaCl, and abscisic acid, and *PCA1* loss-of-function mutants (Δ*PCA1*) exhibit an enhanced susceptibility to salt stress. The Δ*PCA1* lines show sustained elevated $[Ca^{2+}]_{cyt}$ in response to salt treatment in contrast to WT that shows transient Ca^{2+} elevations, indicating a direct role for PCA1 in the restoration of prestimulus $[Ca^{2+}]_{cyt}$. The altered Ca^{2+} response of the Δ*PCA1* mutant lines correlates with altered expression levels of stress-induced genes, suggesting disturbance of a stress-associated signaling pathway. We propose that PCA1 is an essential component for abiotic stress adaptation in *Physcomitrella* involved in the generation of a specific salt-induced Ca^{2+} signature.

abiotic stress | calcium | signaling | targeted knockout

Ca^{2+} is an important second messenger in animals and plants, and changes in cytoplasmic free Ca^{2+} ($[Ca^{2+}]_{cyt}$) are early events in plant signaling pathways, including abiotic stress signaling (1–3). A recent study in *Arabidopsis thaliana* identified genes whose expression was regulated by changes in $[Ca^{2+}]_{cyt}$ where stress-responsive genes were significantly overrepresented, substantiating the role of Ca^{2+} in stress signaling pathways (4).

Rising $[Ca^{2+}]_{cyt}$ levels are caused by increased Ca^{2+} influx (1) or the release of Ca^{2+} from intracellular stores (5) through Ca^{2+}-permeable channels. $[Ca^{2+}]_{cyt}$ is sensed by proteins that are activated upon Ca^{2+} binding such as Ca^{2+}-dependent protein kinases (CDPKs), or by proteins that undergo conformational changes such as calcineurin B-like (CBL) proteins to regulate downstream targets. The transcription of several CDPK genes is induced by abiotic stress (6–8), and *Arabidopsis CPK4* and *CPK11* loss-of-function mutants show pleiotropic abscisic acid (ABA)-insensitive phenotypes and enhanced salt sensitivity (7). Furthermore, *Arabidopsis cpk3* and *cpk6* mutants show impaired ABA- and Ca^{2+}-induced stomatal closing that is correlated with impaired guard cell ion channel regulation (9).

Likewise, CBL genes are up-regulated by abiotic stress factors, and CBL4 and CBL10 act as calcium sensors required for the acquirement of salt tolerance (10–12).

Influx of Ca^{2+} is countered by the removal of Ca^{2+} from the cytoplasm to reconstitute basal $[Ca^{2+}]_{cyt}$. The balance between Ca^{2+} influx and efflux determines the kinetic and temporal nature of the Ca^{2+} elevation. ATP-driven Ca^{2+} pumps (Ca^{2+}-ATPases) and transporters driven by electrochemical gradients, such as Ca^{2+}/H^{+} exchangers, play an important role in maintaining low $[Ca^{2+}]_{cyt}$ (1).

According to their homology to animal counterparts, plant Ca^{2+}-ATPases are subgrouped into types IIA and IIB (13). The latter contain an N-terminal autoinhibitory domain that responds to Ca^{2+} signals by a Ca^{2+}-induced binding of calmodulin, resulting in the activation of the Ca^{2+} pump (14). Even though changes in $[Ca^{2+}]_{cyt}$ are associated with abiotic stress signaling there is as yet only indirect evidence for a role of plant Ca^{2+}-ATPases in stress signaling based on the ABA-responsive expression of the *Arabidopsis* genes *ACA8* and *ACA9* (15) and the acquirement of enhanced osmotolerance of a yeast strain overexpressing the *Arabidopsis ACA4* gene (16). However, transgenic approaches have shown that plant Ca^{2+}-ATPases are involved in other fundamental processes such as pollen tube growth, vegetative development, inflorescence architecture, and gibberellin signaling (17–19). These studies suggest similar fundamental functions of P-type Ca^{2+}-ATPases in plants and animals as the generation of KO mice revealed perturbations upon the targeted ablation of specific Ca^{2+}-ATPases including lethality, tumorigenesis, skin and muscle diseases, deafness, balance disorders, and male infertility (20). It is assumed that these defects rely on the role of animal Ca^{2+}-ATPases in the clearance of $[Ca^{2+}]_{cyt}$, making them critical factors in Ca^{2+}-mediated signaling cascades (21–23).

In bryophytes, changes in $[Ca^{2+}]_{cyt}$ control developmental programs such as caulonema differentiation (24), protoplast division (25), and cytokinin-induced bud formation (26, 27). Changes in $[Ca^{2+}]_{cyt}$ were also reported in response to abiotic stress including mechanical stimulation (28, 29), mechano-relocation of chloroplasts (30), UV-A light exposure (31), and cold (29). Thus, changes in $[Ca^{2+}]_{cyt}$ occur in response to internal and external stimuli in bryophytes, but the constituents that control $[Ca^{2+}]_{cyt}$ in mosses have not yet been identified.

Results

Isolation of *PCA1* from *Physcomitrella*. Cloning of a Ca^{2+}-ATPase was initiated by using a partial 750-bp *Physcomitrella* cDNA homologous to the C-terminal region of P-type Ca^{2+}-ATPases (32). The full-length cDNA was isolated from a cDNA library and

Author contributions: H.H., R.R., and W.F. designed research; E.Q., A.M.C.F., G.W., D.L., and C.B. performed research; E.Q., A.M.C.F., G.W., D.L., H.H., C.B., R.R., and W.F. analyzed data; and W.F. wrote the paper.

The authors declare no conflict of interest.

This article is a PNAS Direct Submission.

Data deposition: The sequences reported in this paper have been deposited in the GenBank database (accession nos. AJ428949, AJ544769, At5g57110, At4g29900, AJ566740, AJ566742, Phypa_74335, and Phypa_173331).

[1]Present address: Merck Biosciences, Ober der Roeth, 65824 Schwalbach, Germany.

[2]To whom correspondence should be addressed. E-mail: wolfgang.frank@biologie.uni-freiburg.de.

This article contains supporting information online at www.pnas.org/cgi/content/full/0800864105/DCSupplemental.

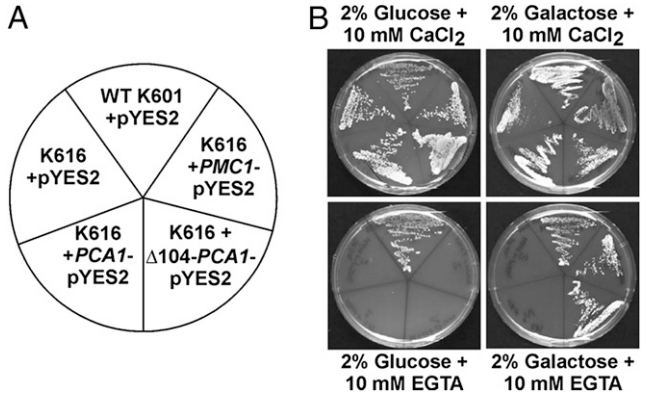

Fig. 1. *PCA1* complements the Ca^{2+} transport-deficient yeast mutant K616. (*A*) Arrangement of the yeast mutant strain K616 and WT strain K601 transformed with different expression constructs. (*B*) Growth of the transformed yeast strains at high (*Upper*) and low (*Lower*) Ca^{2+} concentrations in the presence of galactose (*Right*) or glucose (*Left*).

subsequent amplification of the 5′ end by 5′ RACE-PCR. The cDNA encodes a protein of 1,098 aa and was designated *PCA1* (P-type Ca^{2+}-ATPase 1). Based on the presence of specific sequence motifs PCA1 can be classified as a P_{IIB}-type plant Ca^{2+}-ATPase (Fig. S1). The most striking motif is a calmodulin binding site at the N terminus (amino acids 40–62) that is part of an N-terminal autoinhibitory domain present in P_{IIB}-type Ca^{2+}-ATPases (14). Furthermore, a topology prediction (33) suggests that PCA1 contains 10 membrane spanning domains that are characteristic for this class of Ca^{2+}-ATPases (13). PCA1 also shares the conserved phosphorylation motif DKTGTLT (amino acids 467–473), 2 motifs (PAD and TGES) required for the activation of the protein, and the PEGL motif present in cation transporting Ca^{2+}-ATPases (34). Similar to the *Arabidopsis* P_{IIB}-type Ca^{2+}-ATPase genes *ACA8* and *ACA10*, *Physcomitrella PCA1* contains 34 exons and the exon/intron borders are identical in 30 of 33 positions, suggesting a high conservation of the gene structure in land plants (Fig. S2).

***PCA1* Complements a Ca^{2+} Transport-Deficient Yeast Mutant.** In the yeast *Saccharomyces cerevisiae*, Ca^{2+} homeostasis is maintained by the P-type Ca^{2+}-ATPases PMC1, PMR1, and the Ca^{2+}/H^+ antiporter VCX1 (35) that is inhibited by calcineurin and is not active at low Ca^{2+} concentrations. In the yeast strain K616 (*pmr1*, *pmc1*, *cnb1*) *PMC1*, *PMR1* and the calcineurin subunit *CNB1* are deleted and maintenance of Ca^{2+} homeostasis relies solely on VCX1 activity. At physiological Ca^{2+} concentrations ($\geq$ 1 mM Ca^{2+}) the mutant grows as well as WT, but growth is inhibited at low Ca^{2+} concentrations because of the inactivation of VCX1 (13) and complementation assays in the K616 yeast mutant background are used for the functional analysis of Ca^{2+}-ATPases (14, 16). We cloned the *PCA1* ORF and a truncated *PCA1* cDNA lacking the N-terminal autoinhibitory domain into the yeast expression vector pYES2 (Fig. 1*A* and Fig. S3). The protein derived from the latter construct should not require activation by Ca^{2+}/calmodulin and therefore was expected to be constitutively active. As a positive control, we used the yeast *PMC1* gene encoding a Ca^{2+}-ATPase (35). The expression of the cDNAs was controlled by the *GAL1* promoter that is induced by galactose and repressed by glucose. At high Ca^{2+} concentrations, the strain K616 grew as well as the WT and the expression of any of the cDNAs had no effect on the growth rate (Fig. 1*B*). However, at low Ca^{2+} concentrations in the presence of galactose transformants harboring the truncated *PCA1* or the control *PMC1* cDNA, but not those harboring the full-length *PCA1* cDNA, were able to grow. In the presence of glucose that represses the *GAL1* promoter only the WT grew. These results indicate that

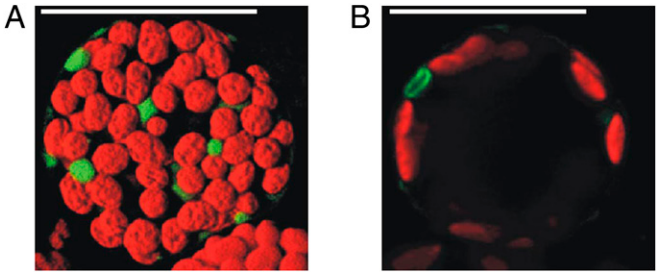

Fig. 2. PCA1 resides in membranes of small vacuoles. (*A*) Overlay of the red chlorophyll and green GFP fluorescence of a protoplast transfected with a *PCA1*:*GFP* C-terminal fusion construct. (*B*) Confocal section of a transformed protoplast. (Scale bars: 25 μm.)

PCA1 displays Ca^{2+}-transporting activity in yeast. Moreover, the growth inhibition of transformants harboring the full-length PCA1 protein suggests that PCA1 presents a P_{IIB}-type Ca^{2+}-ATPase containing an N-terminal autoinhibitory domain.

PCA1 Is Localized to Small Vacuoles. Exploring the intracellular localization of Ca^{2+}-ATPases may provide insights into the subcellular compartments that are involved in the maintenance of low $[Ca^{2+}]_{cyt}$. Previous studies indicated a diverse localization of plant P_{IIB}-type Ca^{2+}-ATPases in the plasma membrane (17, 36), the endoplasmic reticulum (ER) (37), small vacuoles (16), and the central vacuole (38). To analyze the localization of PCA1, we fused the cDNA of the GFP to the 3′ end of the *PCA1* coding region under the control of the cauliflower mosaic virus 35S promoter and transfected the construct into *Physcomitrella* protoplasts that were analyzed by confocal laser scanning microscopy 48 h after the transformation. GFP fluorescence could not be detected at the plasma membrane, the central vacuole, or structures of the ER. However, GFP accumulation was observed in small vacuoles (Fig. 2*A*) and confocal sections indicated that the fusion protein resides in the membranes of these small vacuolar structures (Fig. 2*B*). Thus, the localization of PCA1 is identical to the reported localization of the *Arabidopsis* ACA4 P_{IIB}-type Ca^{2+}-ATPase (16).

***PCA1* Is Induced by Dehydration, Salt, and ABA.** To obtain indications for the function of *PCA1* in the abiotic stress response, mRNA levels were analyzed in response to dehydration, salt, and ABA, which mediates stress-induced gene expression in mosses and seed plants (39). RNA gel blots indicated increased *PCA1* mRNA levels in response to all stimuli (Fig. 3). During dehydration we observed elevated *PCA1* mRNA levels after 4 h that did not change after 8 h. Upon NaCl treatment induction of *PCA1* occurred after 1 h and transcript levels remained high up to 8 h. ABA caused a transient induction of the *PCA1* gene rising up to 4 h, thereafter returning to the basal prestimulus level. From the elevated *PCA1* mRNA levels in response to abiotic stress and ABA we assumed a functional role of PCA1 in abiotic stress adaptation.

Generation of *PCA1* KO Mutants. In *Physcomitrella*, the integration of DNA into its genome by means of homologous recombination facilitates the generation of targeted gene KO lines (40). Southern

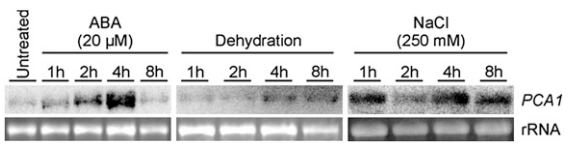

Fig. 3. Expression analysis of *PCA1* in response to ABA, dehydration, and NaCl. (*Upper*) *PCA1* hybridization signals. (*Lower*) Ethidium bromide-stained rRNA bands (loading control).

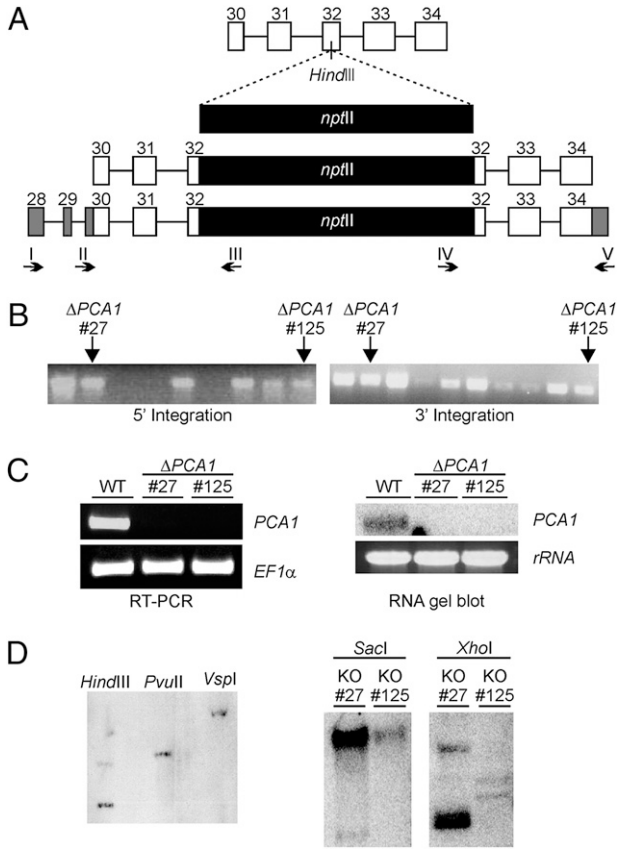

Fig. 4. Generation and molecular analysis of Δ*PCA1* KO lines. (*A*) (*Top*) Insertion of a *nptII* selection marker cassette into a HindIII restriction site in exon 32 of the *PCA1* gene. (*Middle*) Resulting *PCA1* KO construct. (*Bottom*) Genomic structure after integration of the *PCA1* KO construct by homologous recombination. Primers used for the analysis of transgenic lines are indicated by arrows and roman numbers. Black box: *nptII* cassette; open boxes: exon sequences within the KO construct; gray boxes: exons flanking the KO construct. (*B*) PCR analysis to confirm 5′ and 3′ integration of the *PCA1* KO construct. (*Left*) 5′ Integration analysis with primers I and III. (*Right*) 3′ Integration analysis with primers IV and V. PCR products obtained from Δ*PCA1* KO lines 27 and 125 are indicated by arrows. (*C*) (*Left*) RT-PCR analysis with primers II and V (*PCA1*) and primers for the control gene *EF1α*. (*Right*) RNA gel blot hybridized with a *PCA1* probe and ethidium bromide-stained rRNA bands to indicate equal loading. (*D*) (*Left*) Genomic Southern blot from *Physcomitrella* WT DNA digested with the indicated restriction enzymes hybridized with a *PCA1* probe (HindIII cuts once; PvuII and VspI do not cut). (*Right*) Genomic Southern blot with DNA from the Δ*PCA1* mutants 27 and 125 digested with the indicated restriction enzymes and hybridized with the *npt II* selection marker cassette (XhoI cuts once; SacI does not cut).

blot analysis revealed that *PCA1* is a single-copy gene, thus representing a suitable target for a gene disruption approach (Fig. 4*D*). A *PCA1* gene disruption construct was generated by inserting an *nptII* selection marker cassette into the 3′ genomic region of *PCA1* (Fig. 4*A*) and used for the transformation of *Physcomitrella* protoplasts. Regenerating plants were screened for a disrupted *PCA1* locus by performing PCR on genomic DNA of transgenic lines with primers flanking the expected integration site in combination with primers derived from the 35S promoter and 35S terminator sequences present in the *nptII* cassette. PCR products of the expected size were amplified from independent transgenic lines demonstrating the disruption of the *PCA1* genomic locus by precise 5′ integration and 3′ integration events. Two lines (Δ*PCA1*27 and Δ*PCA1*125) were selected for further analysis (Fig. 4*B*). RT-PCR and RNA gel blot analyses did not detect a *PCA1* transcript in the 2 Δ*PCA1* mutant lines, but did in WT (Fig. 4*C*), verifying the generation of *PCA1* loss-of-function mutants. To determine the number of integration sites of the *PCA1* KO construct the 2 Δ*PCA1* mutant lines were subjected to genomic Southern blot analysis using the *nptII* selection marker cassette as hybridization probe. The resulting hybridization patterns demonstrate 1 integration event of the *nptII* cassette in the mutant Δ*PCA1*125 and 2 integration events in the mutant Δ*PCA1*27 (Fig. 4*D*). Furthermore, we analyzed both Δ*PCA1* mutants by flow cytometry to exclude the generation of diploid lines by protoplast fusion during the transformation process. Both KO lines were shown to be haploid as was the WT (data not shown).

***PCA1* KO Lines Display Decreased Salt Tolerance.** To investigate phenotypic effects caused by the disruption of the *PCA1* gene, the 2 Δ*PCA1* mutant lines were compared with *Physcomitrella* WT plants on standard growth medium. We did not observe any difference in growth rate or developmental progression. Likewise, the addition of auxin or cytokinin that are known to cause changes in $[Ca^{2+}]_{cyt}$ in moss (24–27) did not reveal any differences between WT and the Δ*PCA1* mutants, suggesting that PCA1 is not involved in the regulation of development. Because Ca^{2+} is a second messenger in abiotic stress responses and *PCA1* mRNA levels were stress-induced, we extended the functional studies of the Δ*PCA1* mutants to growth experiments on medium supplemented with NaCl. Both Δ*PCA1* mutant lines and WT plants were grown on medium containing 500 mM NaCl, and the salt tolerance was assessed by monitoring the degree of bleaching of the plants and the measurement of cell death (Fig. 5 *A–D*). After 3 days, the 2 Δ*PCA1* mutant lines showed enhanced bleaching compared with WT plants (Fig. 5*B*). Also, after 6 days the Δ*PCA1* mutants were more susceptible to salt stress as indicated by partial bleaching of the majority of plants and complete bleaching of single plants, whereas most WT plants remained green and only a few plants showed partial bleaching (Fig. 5*C*). These apparent deviating phenotypes revealed significant differences between the WT and the 2 Δ*PCA1* mutant lines. In addition, we determined cell death rates in the 2 Δ*PCA1* mutants and WT plants by Evans blue staining that is indicative for loss of plasma membrane integrity (41). Δ*PCA1* mutants and WT were grown in liquid medium containing 500 mM NaCl. According to the phenotypic analysis the 2 Δ*PCA1* mutant lines displayed higher cell death rates upon NaCl treatment compared with WT plants (Fig. 5*D*). The different degree of chlorosis during the NaCl treatment in WT and the Δ*PCA1* mutants should have a direct effect on photosynthesis rates that can be determined by chlorophyll fluorescence measurements (42). Liquid cultures of WT and the Δ*PCA1*125 mutant were grown at different NaCl concentrations (200, 300, 400, and 500 mM NaCl), and the maximum quantum yield of photosystem II was measured 12, 24, and 48 h after the beginning of the treatment. Both WT and the Δ*PCA1*125 mutant line showed a concentration and time-dependent decrease in the photosynthesis rate in the presence of elevated NaCl concentrations (Fig. 5*E*). Furthermore, the Δ*PCA1*125 mutant line exhibited lower maximum quantum yields compared with WT, which became most evident after 48 h of salt treatment. The reduced photosynthesis rates in the Δ*PCA1* mutant in relation to WT correspond to the enhanced chlorosis observed in the phenotypic analysis, providing further evidence for the reduced salt tolerance of the Δ*PCA1* mutant lines. Based on these results we infer that *PCA1* is essential for salt stress adaptation in *Physcomitrella*.

Δ*PCA1* Mutants Fail to Restore Resting Ca^{2+} Levels After Salt Stress Treatments and Display Disturbed Expression of Stress-Induced Genes. To test a direct role of PCA1 in salt stress adaptation, we measured changes in $[Ca^{2+}]_{cyt}$ in response to NaCl in *Physcomitrella* WT and the mutant line Δ*PCA1*125. $[Ca^{2+}]_{cyt}$ was measured ratiometrically after biolistic delivery of the Ca^{2+}-sensitive dye Oregon Green 488 BAPTA dextran and the Ca^{2+}-insensitive

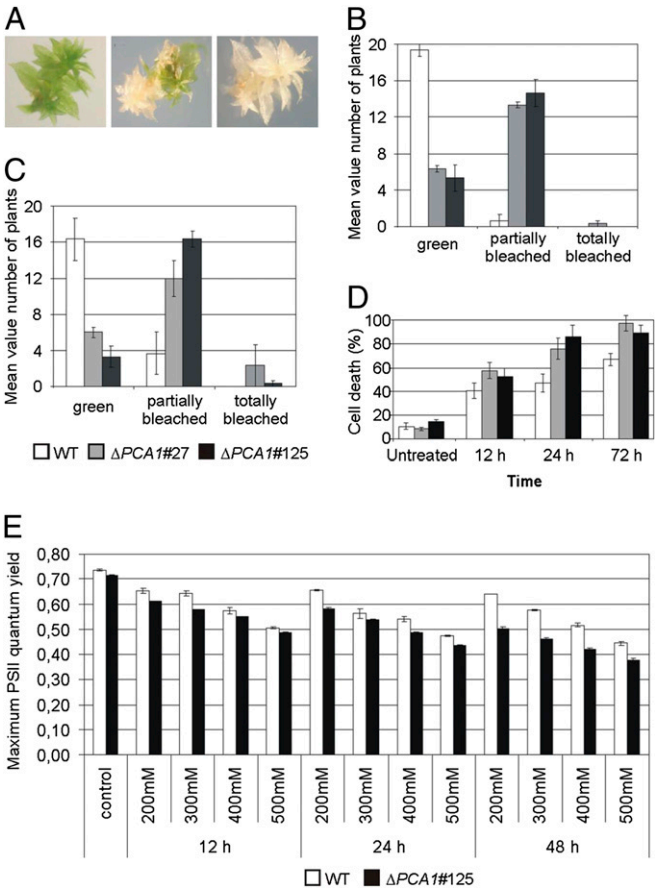

Fig. 5. Δ*PCA1* mutant lines are more susceptible to NaCl stress. (*A*) Δ*PCA1* mutants and WT grown on solid medium with 500 mM NaCl. Exemplary pictures depict the 3 phenotypic categories. (*B* and *C*) The phenotype of plants was recorded after 3 (*B*) and 6 days (*C*) of NaCl treatment. (*D*) Cell death measurement in WT plants and Δ*PCA1* mutant lines by Evans blue staining after growth in liquid medium containing 500 mM NaCl. Error bars indicate standard errors of 3 independent experiments. (*E*) Measurement of photosystem II (PSII) maximum quantum yield in WT and the Δ*PCA1*125 mutant in response to different NaCl concentrations.

Cascade Blue dextran into protonema cells (43) (Fig. 6*A*). We detected similar basal $[Ca^{2+}]_{cyt}$ in WT and the Δ*PCA1*125 mutant line. In WT, the perfusion with 250 mM NaCl caused a transient peak in $[Ca^{2+}]_{cyt}$ that reached a maximum of ≈200 nM after 120 s and returned to prestimulus levels within 5 min. In contrast, in the Δ*PCA1*125 mutant $[Ca^{2+}]_{cyt}$ increased up to 500 nM 110 s after the NaCl perfusion and did not return to prestimulus levels within the investigated time period (Fig. 6*B*, Fig. S4, Table S1). Thus, PCA1 activity modulates both the amplitude and the duration of the Ca^{2+} elevation in response to salt stress. We further hypothesized that the disturbed Ca^{2+} signature may affect the transmission of the stress signal at different levels including the activation of stress-responsive genes. To test this scenario, we analyzed mRNA levels of stress-responsive genes after the application of NaCl and ABA in WT and Δ*PCA1* mutants. Two genes encoding a dehydrin protein (*PpCOR47*) and a membrane pore protein (*PpCOR-TMC-AP3*) were characterized as stress-inducible genes (39). The Δ*PCA1* mutants and WT were treated with 10 μM ABA and 250 mM NaCl, respectively, and mRNA levels of both genes were monitored in 3 independent biological replicates by RNA gel blots. In WT and both Δ*PCA1* mutant lines transcript levels of the genes increased after 1-h exposure to NaCl and ABA (Fig. 6 *C* and *D* and Table S2). In addition, after 1 h the mRNA levels observed in the 2 Δ*PCA1* mutant lines were comparable to those in WT with the exception of slightly increased mRNA levels of *PpCOR-TMC-AP3* in WT plants in response to ABA. However, 3 h after the ABA and NaCl treatment transcript levels were significantly lower in the Δ*PCA1* mutants compared with WT (Fig. 6 *C* and *D* and Table S2). In *Arabidopsis*, it was suggested that ABA-responsive elements (ABRE) within promoter regions mediate Ca^{2+}-responsive gene expression (4). Also in *Physcomitrella*, ABREs are functional *cis*-elements conferring stress-induced gene expression (44, 45). To test whether ABREs are present in the genes *PpCOR47* and *PpCOR-TMC-AP3*, we analyzed their promoter regions. In fact, we identified putative ABREs in the promoter regions of both genes, suggesting that these elements may transmit changes in $[Ca^{2+}]_{cyt}$ in *Physcomitrella* (Fig. 6*E*). According to the empirical cumulative distribution of all ABRE matches in the 1.5-kb upstream regions of all 27,962 *Physcomitrella* V1.2 gene models (46) (Fig. S5), the overrepresentation of ABREs was found to be significant [$P_{(x >= 6)} = 0.00021$; $P_{(x >= 7)} = 7 \times 10^{-05}$]. The promoter of *PCA1*, which is transiently induced by ABA, does not harbor ABREs, suggesting that the expression might be controlled by a different pathway. We further analyzed whether the application of exogenous Ca^{2+} is able to mimic the stress induction of *PpCOR47* and *PpCOR-TMC-AP3*. WT plants were grown in medium with 100 nM $CaCl_2$, which corresponds to the basal $[Ca^{2+}]_{cyt}$ and subsequently $CaCl_2$ was added at concentrations of 1 and 5 mM. For both genes, we did not detect considerable changes in mRNA steady-state levels in response to applied Ca^{2+}, which may resemble the stress-induced expression pattern of the genes in response to NaCl or ABA (Fig. S6). Thus, application of exogenous Ca^{2+} is not sufficient to activate the stress signaling pathway(s) regulating *PpCO47* and *PpCOR-TMC-AP3*. Taken together, the perturbation of the salt-induced Ca^{2+} signal and the deregulation of stress-induced genes in the Δ*PCA1* mutant lines suggest a function of PCA1 in stress signaling.

Discussion

The stimulus-dependent generation of $[Ca^{2+}]_{cyt}$ transients has been intensively studied (47), but experimental data on the proteins that restore $[Ca^{2+}]_{cyt}$ are scarce. Ca^{2+}-ATPases are thought to be the major components regulating $[Ca^{2+}]_{cyt}$ homeostasis. *Physcomitrella* PCA1 contains all characteristic motifs of plant P_{IIB}-type Ca^{2+}-ATPases, and its Ca^{2+}-transport activity was substantiated by a yeast complementation where PCA1 displayed an identical mode of action already described for other plant P_{IIB}-type Ca^{2+}-ATPases (14, 16, 17).

To date, there are only 2 reported *Arabidopsis* P_{IIB}-type Ca^{2+}-ATPase gene KO lines, where the disruption of *ACA9* caused partial male sterility, and disruption of *ACA10* led to defects in vegetative growth and inflorescence architecture (17, 19). Nevertheless, the expression pattern of other Ca^{2+}-ATPase genes in *Arabidopsis* suggested a function of Ca^{2+}-ATPases in abiotic stress-related pathways (15). Likewise, *PCA1* is regulated by an ABA-dependent stress signaling pathway. Moreover, the reduced tolerance of the Δ*PCA1* mutants to salt provides genetic evidence for its role in salt stress adaptation, and the reduced mRNA levels of stress-induced genes in response to salt and ABA suggest that they are controlled by a signaling pathway requiring PCA1 activity. Evidence that plant Ca^{2+}ATPases are positive regulators of signaling pathways was obtained from the overexpression of a gibberellin-responsive Ca^{2+}-ATPase in rice aleurone cells that caused induction of a gibberellin-responsive α-amylase gene in the absence of gibberellin (18).

The Δ*PCA1* mutants fail to generate a salt-induced transient Ca^{2+} peak and exhibit elevated $[Ca^{2+}]_{cyt}$. One could expect that the elevated $[Ca^{2+}]_{cyt}$ leads to an enhanced Ca^{2+} response and finally results in elevated transcript levels of genes controlled by this pathway. Actually, loss of *PCA1* resulted in decreased transcript levels of stress-responsive genes. We therefore propose that PCA1 is required to restore the $[Ca^{2+}]_{cyt}$ for the generation of a stimulus-

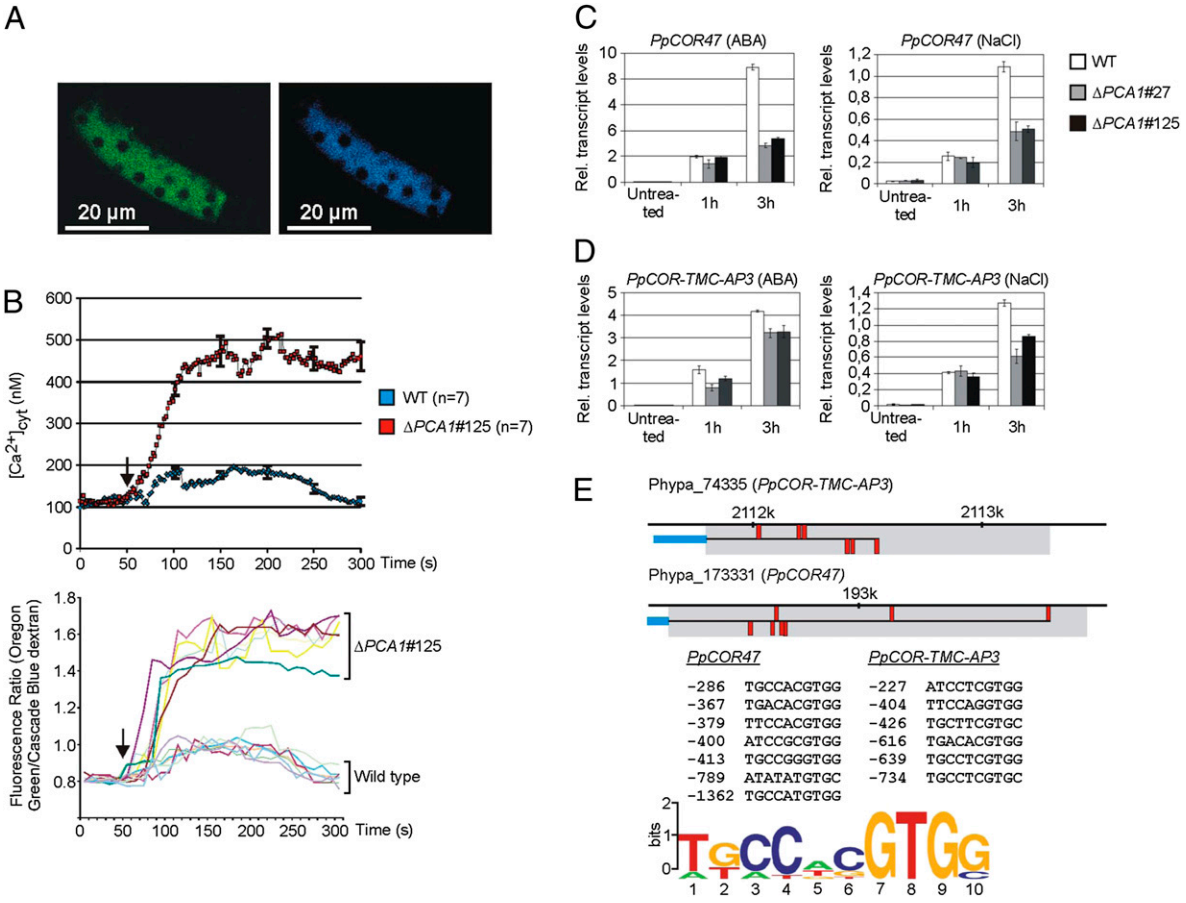

Fig. 6. Measurement of $[Ca^{2+}]_{cyt}$ and expression analysis of stress-induced genes in response to NaCl. (*A*) Exemplary images of a *Physcomitrella* cell loaded with Oregon Green 488 BAPTA dextran (*Left*) and Cascade Blue dextran (*Right*) (*B*) Measurement of $[Ca^{2+}]_{cyt}$ in *Physcomitrella* WT plants and the Δ*PCA1*125 mutant. (*Upper*) Mean values of 7 independent measurements. Error bars indicate standard errors calculated for each 50 s after the addition of NaCl. Statistical significance analysis is shown in Table S1. (*Lower*) Complete graphs of $[Ca^{2+}]_{cyt}$ profiles of 7 independent measurements in WT and the Δ*PCA1*125 mutant in response to 250 mM NaCl. The black arrows indicate the addition of 250 mM NaCl. A typical fluorescence time course of both dyes is shown in Fig. S4. (*C* and *D*) Expression analysis of *PpCOR47* (*C*) and *PpCOR-TMC-AP3* (*D*) in WT and Δ*PCA1* mutants 27 and 125 in response to 250 mM NaCl and 10 μM ABA. The diagrams depict mean values of relative transcript levels from 3 independent experimental replicates; error bars depict standard errors. Expression raw data are shown in Table S2. (*E*) Analysis of ABRE elements in the promoters of *PpCOR47* and *PpCOR-TMC-AP3*. (*Top*) Blue horizontal line: start of coding sequence; gray area: 1.5-kb upstream region subjected to the motif analysis; red boxes: ABRE elements; numbers above indicate nucleotide positions of genomic scaffolds. (*Middle*) Individual ABRE sequences in the promoter regions of *PpCOR47* and *PpCOR-TMC-AP3*. (*Bottom*) Visualization of ABRE consensus sequences as a sequence logo.

specific transient increase in $[Ca^{2+}]_{cyt}$ (3, 47) that is required for the transmission of the initial stress signal. Substantial evidence that Ca^{2+}-ATPases are in fact key regulators of $[Ca^{2+}]_{cyt}$ was provided in animal cells where Ca^{2+}-ATPases are indispensable for the restoration of basal $[Ca^{2+}]_{cyt}$ and required for proper signal transmission (21–23). It is plausible that altered Ca^{2+} signatures affect the activation of Ca^{2+} sensor proteins, resulting in perturbed downstream signaling steps.

PCA1 was localized in membranes of small vacuolar compartments, which is consistent with the localization of the *Arabidopsis* P_{IIB}-type Ca^{2+}-ATPase ACA4 (16). The additional subcellular localization sites of plant P_{IIB}-type Ca^{2+}-ATPases in the plasma membrane (17, 36), the ER (37), and the central vacuole (38) point to functional diversities within the plasma membrane and the endomembrane system in relation to Ca^{2+} homeostasis and Ca^{2+} signaling. Besides Ca^{2+}-ATPases, Ca^{2+}/H^+ exchangers control Ca^{2+} homeostasis under stress conditions as *Arabidopsis* T-DNA mutants of the *CAX1* Ca^{2+}/H^+ antiporter displayed an enhanced freezing tolerance that was correlated with an elevated expression of *CBF*/*DREB1* genes and their corresponding targets (48). Furthermore, *Arabidopsis cax1* and *cax3* mutants display an increased sensitivity to ABA and sugar during seed germination and an increased tolerance to ethylene (49). CAX1 and CAX3 were also found to play a role in plant growth and nutrient acquisition (50). Furthermore, it was suggested that CAX3 is the predominant Ca^{2+}/H^+ antiporter in *Arabidopsis* under salt stress conditions, whereas CAX1 is essentially inactive, which is correlated with their expression as CAX3 is up-regulated by salt but CAX1 is not (49).

Compared with elevated mRNA levels of stress-responsive genes in the *Arabidopsis cax1* mutant, the reduced expression of stress-responsive genes in the *Physcomitrella* Δ*PCA1* mutants suggests that the action of Ca^{2+}/H^+ antiporters and Ca^{2+} pumps lead to different responses in signaling pathways. In addition, the disruption of the *Arabidopsis* genes *ACA9* and *ACA10* (17, 19) and the deletion of the *Physcomitrella PCA1* cause distinct phenotypes. However, the alterations are found in completely different biological pathways, namely developmental programs in *Arabidopsis* and abiotic stress signaling in *Physcomitrella*, suggesting that plant Ca^{2+}-ATPases have distinct biological functions.

Materials and Methods

Plant Material. *P. patens* was cultured as described (39, 51). Detailed descriptions of the phenotypic analysis, treatments with ABA and NaCl, and the application of exogenous Ca^{2+} are provided in *SI Text*.

Molecular Cloning and Analysis of Transgenic *Physcomitrella* Lines. A detailed description of the DNA constructs used in this study and the molecular analyses of the generated transgenic *Physcomitrella* lines are provided in *SI Text*.

Yeast Complementation. The transformation of yeast cells was performed according to Ausubel *et al.* (52). Transformed cells were plated onto SDLHAW plates that were supplemented with 2% glucose/10 mM $CaCl_2$, 2% glucose/10 mM EGTA, 2% galactose/10 mM $CaCl_2$, or 2% galactose/10 mM EGTA.

RNA and DNA Blot Hybridization. RNA blot hybridization was carried out as described (39) with the following radioactively labeled cDNA probes: *PpCOR47*, *PpCOR-TMC AP3* (39), the homolog to ribosomal protein L21 (32) amplified from cDNA with the primers 5′-GGTTGGTCATGGGTTGCG-3′ and 5′-GAGGTCAACTGTCTCGCC-3′, and a *PCA1* cDNA fragment amplified using the primers 5′-TTGCGATTGGCTTCATAAGCTG-3′ and 5′-ACGGTAAAAGACAACGATCAAGTT-3′. Signal intensities were quantified by using the Quantity One software package (BioRad). *PpCOR47* and *PpCOR-TMC-AP3* transcript levels were normalized to the constitutive control L21 mRNA. Mean values from 3 biological replicates and standard errors were calculated. Genomic DNA was digested with the indicated restriction enzymes, blotted, and hybridized with a *PCA1* cDNA fragment (analysis of *PCA1* gene copy number) or the *nptII* selection marker cassette present in the *PCA1* gene disruption construct (analysis of integrations in the Δ*PCA1* mutants).

Measurement of Cytosolic Calcium. $[Ca^{2+}]_{cyt}$ was measured ratiometrically after biolistic delivery of the Ca^{2+}-sensitive dye Oregon Green 488 BAPTA dextran and the Ca^{2+}-insensitive Cascade Blue dextran into *Physcomitrella* cells as described (43). A detailed description of the method is provided in *SI Text*.

Promoter Analysis. Regions (1.5 kb) upstream of the translation start of the *PpCOR47* and *PpCOR-TMC-AP3* gene models V1.2 (46) were extracted and screened for overrepresented motifs by the Gibbs sampling algorithm as implemented in AlignACE (53). The resulting overrepresented motifs were compared with the ABRE consensus sequence of seed plants (4, 54). Significance was tested by using the empirical cumulative distribution of all ABRE matches in the 1.5-kb upstream regions of all 27,962 V1.2 gene models, and probability values [$P_{(x >= N)}$] for the occurrence of the observed ABRE frequencies (N) in the genes *PpCOR47* and *PpCOR-TMC-AP3* were calculated.

ACKNOWLEDGMENTS. We thank M. Palmgren (University of Copenhagen) for yeast strains K601/W303–1A and K616, G. Fink (Whitehead Institute for Biomedical Research) for the *PMC1* cDNA, and M. Vervliet for help in photosystem II quantum yield measurements. This work was supported by Deutsche Forschungsgemeinschaft Grants RE837/6-3 (to W.F.) and RE827/10 (to R.R.), German Federal Ministry of Education and Research Grant 0313921 (to W.F. and R.R.), Excellence Initiative of the German Federal and State Governments Grant EXC 294 (to R.R.), and the German Academic Exchange Service (Ph.D fellowship to E.Q.).

1. Hetherington AM, Brownlee C (2004) The generation of Ca^{2+} signals in plants. *Annu Rev Plant Biol* 55:401–427.
2. Sanders D, Pelloux J, Brownlee C, Harper JF (2002) Calcium at the crossroads of signaling. *Plant Cell* 14 (Suppl):S401–S417.
3. Scrase-Field SA, Knight MR (2003) Calcium: Just a chemical switch? *Curr Opin Plant Biol* 6:500–506.
4. Kaplan B, *et al.* (2006) Rapid transcriptome changes induced by cytosolic Ca^{2+} transients reveal ABRE-related sequences as Ca^{2+}-responsive *cis* elements in *Arabidopsis*. *Plant Cell* 18:2733–2748.
5. Peiter E, *et al.* (2005) The vacuolar Ca^{2+}-activated channel TPC1 regulates germination and stomatal movement. *Nature* 434:404–408.
6. Ray S, *et al.* (2007) Expression analysis of calcium-dependent protein kinase gene family during reproductive development and abiotic stress conditions in rice (*Oryza sativa* L. ssp. indica). *Mol Genet Genomics* 278:493–505.
7. Zhu SY, *et al.* (2007) Two calcium-dependent protein kinases, CPK4 and CPK11, regulate abscisic acid signal transduction in *Arabidopsis*. *Plant Cell* 19:3019–3036.
8. Abbasi F, *et al.* (2004) OsCDPK13, a calcium-dependent protein kinase gene from rice, is induced by cold and gibberellin in rice leaf sheath. *Plant Mol Biol* 55:541–552.
9. Mori IC, *et al.* (2006) CDPKs CPK6 and CPK3 function in ABA regulation of guard cell S-type anion- and Ca^{2+}-permeable channels and stomatal closure. *PLoS Biol* 4:e327.
10. Liu J, Zhu JK (1998) A calcium sensor homolog required for plant salt tolerance. *Science* 280:1943–1945.
11. Kim BG, *et al.* (2007) The calcium sensor CBL10 mediates salt tolerance by regulating ion homeostasis in *Arabidopsis*. *Plant J* 52:473–484.
12. Gong D, Guo Y, Schumaker KS, Zhu JK (2004) The SOS3 family of calcium sensors and SOS2 family of protein kinases in *Arabidopsis*. *Plant Physiol* 134:919–926.
13. Geisler M, Axelsen KB, Harper JF, Palmgren MG (2000) Molecular aspects of higher plant P-type Ca^{2+}-ATPases. *Biochim Biophys Acta* 1465:52–78.
14. Hwang I, Harper JF, Liang F, Sze H (2000) Calmodulin activation of an endoplasmic reticulum-located calcium pump involves an interaction with the N-terminal autoinhibitory domain. *Plant Physiol* 122:157–168.
15. Cerana M, *et al.* (2006) Abscisic acid stimulates the expression of two isoforms of plasma membrane Ca^{2+}-ATPase in *Arabidopsis thaliana* seedlings. *Plant Biol* 8:572–578.
16. Geisler M, *et al.* (2000) The ACA4 gene of *Arabidopsis* encodes a vacuolar membrane calcium pump that improves salt tolerance in yeast. *Plant Physiol* 124:1814–1827.
17. Schiott M, *et al.* (2004) A plant plasma membrane Ca^{2+} pump is required for normal pollen tube growth and fertilization. *Proc Natl Acad Sci USA* 101:9502–9507.
18. Chen X, Chang M, Wang B, Wu B (1997) Cloning of a Ca^{2+}-ATPase gene and the role of cytosolic Ca^{2+} in the gibberellin-dependent signaling pathway in aleurone cells. *Plant J* 11:363–371.
19. George L, Romanowsky SM, Harper JF, Sharrock RA (2008) The ACA10 Ca^{2+}-ATPase regulates adult vegetative development and inflorescence architecture in *Arabidopsis*. *Plant Physiol* 146:716–728.
20. Prasad V, Okunade GW, Miller ML, Shull GE (2004) Phenotypes of SERCA and PMCA knockout mice. *Biochem Biophys Res Commun* 322:1192–1203.
21. Foggia L, *et al.* (2006) Activity of the hSPCA1 Golgi Ca^{2+} pump is essential for Ca^{2+}-mediated Ca^{2+} response and cell viability in Darier disease. *J Cell Sci* 119:671–679.
22. Beauvois MC, *et al.* (2006) Glucose-induced mixed $[Ca^{2+}]$c oscillations in mouse β cells are controlled by the membrane potential and the SERCA3 Ca^{2+}-ATPase of the endoplasmic reticulum. *Am J Physiol* 290:C1503–C1511.
23. Periz G, Fortini ME (1999) Ca^{2+}-ATPase function is required for intracellular trafficking of the Notch receptor in *Drosophila*. *EMBO J* 18:5983–5993.
24. Bhatla SC, Haschke HP, Hartmann E (2003) Distribution of activated calmodulin in the chloronema tip cells of the moss *Funaria hygrometrica*. *J Plant Physiol* 160:469–474.
25. Bhatla SC, Kiessling J, Reski R (2002) Observation of polarity induction by cytochemical localization of phenylalkylamine-binding sites in regenerating protoplasts of the moss *Physcomitrella patens*. *Protoplasma* 219:99–105.
26. Saunders MJ, Hepler PK (1983) Calcium antagonists and calmodulin inhibitors block cytokinin-induced bud formation in *Funaria*. *Dev Biol* 99:41–49.
27. Hahm SH, Saunders MJ (1991) Cytokinin increases intracellular Ca^{2+} in *Funaria*: detection with Indo-1. *Cell Calcium* 12:675–681.
28. Haley A, *et al.* (1995) Effects of mechanical signaling on plant cell cytosolic calcium. *Proc Natl Acad Sci USA* 92:4124–4128.
29. Russell AJ, *et al.* (1996) The moss, *Physcomitrella patens*, transformed with apoaequorin cDNA responds to cold shock, mechanical perturbation, and pH with transient increases in cytoplasmic calcium. *Transgenic Res* 5:167–170.
30. Sato Y, Wada M, Kadota A (2003) Accumulation response of chloroplasts induced by mechanical stimulation in bryophyte cells. *Planta* 216:772–777.
31. Tucker EB, *et al.* (2005) UV-A induces two calcium waves in *Physcomitrella patens*. *Plant Cell Physiol* 46:1226–1236.
32. Reski R, *et al.* (1998) Moss (*Physcomitrella patens*) expressed sequence tags include several sequences which are novel for plants. *Bot Acta* 111:145–151.
33. von Heijne G (1992) Membrane protein structure prediction: Hydrophobicity analysis and the positive-inside rule. *J Mol Biol* 225:487–494.
34. Evans DE, Williams LE (1998) P-type calcium ATPases in higher plants: Biochemical, molecular, and functional properties. *Biochim Biophys Acta* 1376:1–25.
35. Cunningham KW, Fink GR (1994) Ca^{2+} transport in *Saccharomyces cerevisiae*. *J Exp Biol* 196:157–166.
36. Bonza MC, *et al.* (2000) At-ACA8 encodes a plasma membrane-localized calcium-ATPase of *Arabidopsis* with a calmodulin-binding domain at the N terminus. *Plant Physiol* 123:1495–1506.
37. Hong B, *et al.* (1999) Identification of a calmodulin-regulated Ca^{2+}-ATPase in the endoplasmic reticulum. *Plant Physiol* 119:1165–1176.
38. Lee SM, *et al.* (2007) Identification of a calmodulin-regulated autoinhibited Ca^{2+}-ATPase (ACA11) that is localized to vacuole membranes in *Arabidopsis*. *FEBS Lett* 581:3943–3949.
39. Frank W, Ratnadewi D, Reski R (2005) *Physcomitrella patens* is highly tolerant against drought, salt, and osmotic stress. *Planta* 220:384–394.
40. Reski R (1998) *Physcomitrella* and *Arabidopsis*: The David and Goliath of reverese genetics. *Trends Plants Sci* 3:209–210.
41. Guo FQ, Crawford NM (2005) *Arabidopsis* nitric oxide synthase1 is targeted to mitochondria and protects against oxidative damage and dark-induced senescence. *Plant Cell* 17:3436–3450.
42. Zhang L, Xing D (2008) Rapid determination of the damage to photosynthesis caused by salt and osmotic stresses using delayed fluorescence of chloroplasts. *Photochem Photobiol Sci* 7:352–360.
43. Bothwell JH, *et al.* (2006) Biolistic delivery of Ca^{2+} dyes into plant and algal cells. *Plant J* 46:327–335.
44. Kamisugi Y, Cuming AC (2005) The evolution of the abscisic acid response in land plants: Comparative analysis of group 1 LEA gene expression in moss and cereals. *Plant Mol Biol* 59:723–737.
45. Knight CD, *et al.* (1995) Molecular responses to abscisic acid and stress are conserved between moss and cereals. *Plant Cell* 7:499–506.
46. Lang D, Zimmer AD, Rensing SA, Reski R (2008) Exploring plant biodiversity: The *Physcomitrella* genome and beyond. *Trends Plants Sci* 13:542–549.
47. Evans NH, McAinsh MR, Hetherington AM (2001) Calcium oscillations in higher plants. *Curr Opin Plant Biol* 4:415–420.
48. Catala R, *et al.* (2003) Mutations in the Ca^{2+}/H^{+} transporter CAX1 increase CBF/DREB1 expression and the cold-acclimation response in *Arabidopsis*. *Plant Cell* 15:2940–2951.
49. Zhao J, *et al.* (2008) The *Arabidopsis* cax3 mutants display altered salt tolerance, pH sensitivity, and reduced plasma membrane H^{+}-ATPase activity. *Planta* 227:659–669.
50. Cheng NH, *et al.* (2005) Functional association of *Arabidopsis* CAX1 and CAX3 is required for normal growth and ion homeostasis. *Plant Physiol* 138:2048–2060.
51. Frank W, Decker EL, Reski R (2005) Molecular tools to study *Physcomitrella patens*. *Plant Biol* 7:220–227.
52. Ausubel F, *et al.* (1994) *Current Protocols in Molecular Biology* (Wiley, New York).
53. Hughes JD, Estep PW, Tavazoie S, Church GM (2000) Computational identification of *cis*-regulatory elements associated with groups of functionally related genes in *Saccharomyces cerevisiae*. *J Mol Biol* 296:1205–1214.
54. Gomez-Porras JL, *et al.* (2007) Genomewide analysis of ABA-responsive elements ABRE and CE3 reveals divergent patterns in *Arabidopsis* and rice. *BMC Genomics* 8:260.

Correction

PLANT BIOLOGY

Correction for "A P_{IIB}-type Ca^{2+}-ATPase is essential for stress adaptation in *Physcomitrella patens*," by Enas Qudeimat, Alexander M. C. Faltusz, Glen Wheeler, Daniel Lang, Colin Brownlee, Ralf Reski, and Wolfgang Frank, which appeared in issue 49, December 9, 2008, of *Proc Natl Acad Sci USA* (105:19555–19560; first published December 2, 2008; 10.1073/pnas.0800864105).

The authors note that Hauke Holtorf should be added to the author line between Daniel Lang and Colin Brownlee. Hauke Holtorf should be credited with designing research and analyzing data. The corrected author line, affiliation line, and author contributions footnote appear below. The online version has been corrected.

Enas Qudeimat[a], Alexander M. C. Faltusz[a], Glen Wheeler[c], Daniel Lang[a], Hauke Holtorf[fb], Colin Brownlee[c], Ralf Reski[a,d,e], and Wolfgang Frank[a,d]

[a]Plant Biotechnology, Institute of Biology II, Faculty of Biology, [d]Freiburg Initiative for Systems Biology, Faculty of Biology, and [e]Centre for Biological Signaling Studies, University of Freiburg, Schänzlestrasse 1, 79104 Freiburg, Germany; [b]Biotechnologisches Gymnasium, Albert-Schweitzer-Schule, 78048 Villingen-Schwenningen, Germany; and [c]Marine Biological Association of the United Kingdom, Citadel Hill, Plymouth PL1 2PB, United Kingdom

Author contributions: H.H., R.R., and W.F. designed research; E.Q., A.M.C.F., G.W., D.L., and C.B. performed research; E.Q., A.M.C.F., G.W., D.L., H.H., C.B., R.R., and W.F. analyzed data; and W.F. wrote the paper.

www.pnas.org/cgi/doi/10.1073/pnas.1116142108

CORRECTION